False-positive incidental lesions detected on contrast-enhanced breast MRI: Clinical and Imaging Features

Afsaneh Alikhassi
University of Toronto Temerty Faculty of Medicine
Xuan Li
University of Toronto Dalla Lana School of Public Health
Frederick Au
University of Toronto Temerty Faculty of Medicine
Supriya Kulkarni
University of Toronto Temerty Faculty of Medicine
Sandeep Ghai
University of Toronto Temerty Faculty of Medicine
Allison Grant
University of Toronto Temerty Faculty of Medicine
VIVIANNE FREITAS (vivianne.freitas@uhn.ca)
University of Toronto Temerty Faculty of Medicine https://orcid.org/0000-0003-2563-0861

Research Article

Keywords: Breast MRI, False positive, breast cancer, biopsy

Posted Date: May 3rd, 2022

DOI: https://doi.org/10.21203/rs.3.rs-1602423/v1

Version of Record: A version of this preprint was published at Breast Cancer Research and Treatment on February 6th, 2023. See the published version at https://doi.org/10.1007/s10549-023-06861-y.

Abstract

Purpose

To identify features of the incidental MRI-detected enhancing lesions associated with false-positive outcomes, impacting patient care.

Methods

Institutional review board-approved retrospective imaging studies and patient's chart review of consecutive asymptomatic women with incidental MRI enhancing lesions detected between January-December 2018, who underwent MRI-guided biopsy. Lesions' frequency and imaging features were recorded, differentiating benign and high-risk lesions. The results were correlated with histopathology as the ground truth or uneventful follow-up of at least one year. Univariate analysis explored correlation between baseline variables and false-positive results.

Results

Two-hundred-nineteen women (median age, 49 years; range, 26–85 years) with 219 incidental MRI enhancing lesions that underwent MRI-guided vacuum-assisted biopsy during the study period formed the study cohort. Out of 219, 180 lesions (82.2%) yielded benign pathology results, 137 benign (76%) and 43 high-risk (24%) outcomes. Variables associated with true-positive results were age OR 1.05 (CI 95%, 1.02–1.08), $p = 0.0015$, irregular compared with oval/round mass shape lesion OR 11.2 (CI 95%, 1.6–78.4), $p = 0.015$, and clumped/clustered ring compared with homogeneous non-mass enhancement OR 3.17 (CI 95%, 1.38–7.28), $p < 0.0066$. T2-hyperintense mass-lesion correlated to the false-positive result OR 0.13 (95% CI, 0.02–0.76), $p = 0.024$.

Conclusion

Young patients, oval/round mass-lesion shape, T2-hyperintense mass-lesion, and homogeneous pattern of non-mass enhancement showed the strongest association with false-positive results of incidental MRI enhancing lesions. It may impact the patient's management, suggesting follow-up rather than interventional procedure when these demographic/imaging parameters are present, consequently decreasing patient's anxiety and health care costs.

Introduction

The use of magnetic resonance imaging (MRI) in breast imaging has increased in recent years, representing an important tool in breast cancer diagnosis, especially in high-risk populations [1–5]. In addition, breast MRI has been discussed as a potential supplemental screening tool for women at

average risk who have dense breast tissue [6–10]. MRI has yielded consistently higher sensitivity and increased cancer detection rates compared with digital mammography (DM) [1–10].

Nevertheless, breast MRI has frequently been reported to result in a large number of false-positive diagnoses. Kuhl, C.K. reported 55.2% false positive in MRI of 366 asymptomatic women with average risk of breast cancer [11]. In principle, all suspicious findings that prompt biopsy but yield nonmalignant tissues are equally considered false positives, which specifically in the breast, is caused by a quite heterogeneous group of tissue changes.

In fact, contrary to what is observed on mammography, the MRI-detected false-positive lesions are usually associated with proliferative results and more high-risk lesions diagnosed, such as atypical ductal hyperplasia and lobular neoplasia [11], for which most practice guidelines recommend intensified surveillance, preventive surgery, or even chemoprevention [12]. Thus, although their diagnosis may provide valuable information to guide further patient management, such false-positive diagnoses add to the overall cost of screening because they require additional workup by imaging or biopsy, may cause physical harm because of additional morbidity associated with biopsy procedures, and may cause emotional harm because they may generate breast cancer anxiety in the patient [13–16]. Accordingly, the reported high number of false-positive diagnoses has been a major reason for limiting the acceptance of breast MRI as a screening tool [17–19].

The review of the literature reveals that there are several articles on sensitivity, specificity and false positive rate of breast MRI, but few studies with conflicting results focused on evaluating lesion characteristics associated with false-positive results [20, 21]. For example, Batzer et al. [20] showed that non-mass-like lesions are more associated with false-positive results, while Myers et al. [21] did not show this association. Furthermore, the larger tumor diameter of the lesion despite the lesion type shows association with malignancy in the Myers study [21] but was only confirmed for mass lesions in the Batzer study [20]. As such, these discrepant results highlight the need for additional studies in this setting. Over time, machines and software have also developed, potentially affecting results.

Recently, several investigators have developed computer aided and machine learning methods for diagnosis and the quantitative characterization of breast lesions on clinical images. Radiomics, a computer-aided diagnosis provides computer-extracted characteristics of tumor. Although some studies showed that artificial intelligence and Radiomics systems improved radiologists' performance in differentiating benign and malignant enhancing lesions detected at breast MRI, most AI methods are still in the technical development and research phase and many efforts should be taken for clinical translation. In addition, they are not widely available worldwide [22–24].

Therefore, this study aims to identify demographic characteristics and imaging findings, including morphological appearance and kinetic pattern of enhancement of the incidental MRI-detected enhancing lesions related to false-positive results. These findings will potentially help reduce the overall cost associated with MRI additional workup and patient harm.

Methods

Patient selection

Consecutive data of patients with MRI-detected enhancing lesions who have undergone MRI-guided percutaneous biopsy in 2018 from three tertiary hospitals: Sinai Health System, University Health Network, and Women's College Hospital, affiliated with the University of Toronto were retrospectively reviewed. The patient's informed consent was waived. Only those who have undergone surgical excision or were followed clinically or by imaging for at least one year from the date of the last imaging examination were included.

All patients had ultrasound or mammography before MRI, but the included lesions did not have mammography or ultrasound correlated lesions. The included lesions had BIRADS 4 or 5 in enhanced MRI, which make them candidate for MRI guided biopsy. Patient's demographics and MRI findings, imaging-guided biopsy results, and if applicable, the pathological outcome after excisional surgery were reviewed.

Imaging technique

MRI was performed using state-of-the-art equipment and standard-of-care technique following American College of Radiology (ACR) quality standards [25]. In all cases, MRI examinations were performed on a 1.5-T system (Signa Excite, GE Medical Systems) or Espree or Avanto (Siemens Healthcare) and 3.0-T system (Verio; Siemens Healthcare) with a standard, bilateral, dedicated breast coil (Sentinelle Vanguard; Sentinelle Medical, Inc.). The sequences included precontrast axial T1, T2-weighted images with fat suppression, and dynamic contrast-enhanced (DCE) T1-weighted imaging sequences. The DCE sequence consisted of a pre-contrast scan and four post-contrast scans. MRI examinations for premenopausal patients were scheduled in the second week of the menstrual cycle to minimize enhancement of benign breast parenchyma (25).

Imaging interpretation

All MRI data were reviewed by two breast fellowship-trained radiologists (AA,12 years of experience, VF, 20 years of experience) from the same department that were blinded to the surgical or core needle biopsy pathology results and the clinical outcomes. The readers described MRI findings following the Breast Imaging Reporting and Data System (BIRADS) lexicon [25, 26]. Discrepant results of lesion characteristics between radiologists were assessed by consensus. The imaging studies with final assessment category BI-RADS 4 and BI-RADS 5 were considered positive, and all other results were considered negative.

Demographic data were recorded, including age, personal history of breast cancer, risk factors including genetic mutation, and family history of breast cancer. In addition, the MRI indication (screening; staging; surveillance; problem-solving; others) and imaging findings were retrieved (parenchymal enhancement; T1 signal, T2 signal, mass or non-mass enhancement; shape and margin for masses; and enhancement pattern and distribution for non-mass enhancement, and dynamic pattern).

Interventional procedures and pathology

Percutaneous MRI-guided biopsies were performed by attending breast imaging experienced radiologists at the same hospital within 3 weeks from the enhanced MR, using a 9-gauge MRI-compatible vacuum-assisted device (ATEC, Suros Surgical systems), with 8 to 12 samples obtained.

Histopathology

The histopathologic result from the MRI-guided biopsy was considered the reference standard for lesion evaluation. Invasive cancer and ductal carcinoma *in situ* (DCIS) were considered malignant histopathological results. The histological results, including papillary lesions, complex sclerosing lesions (CCL), radial scar (RS), atypical ductal hyperplasia (ADH), atypical lobular hyperplasia (ALH), and lobular carcinoma *in situ* (LCIS) were categorized as high-risk lesions (HRL). Other pathologies are considered benign (fibrocystic changes, Pseudoangiomatous stromal hyperplasia, columnar cell changes or hyperplasia, focal fibroadenomatoid changes, stromal fibrosis). Patients with malignancy had surgical excision as per standard institutional practice. In addition, surgery was performed in some of biopsy-proven high-risk lesions, and benign pathology after multidisciplinary discussion, and based on patient's and surgeon preferences.

All included women who did not undergo excisional surgery had a minimum of 12-month follow-up. The standard follow-up was a clinical exam, mammogram alone, or mammogram supplemented by MRI.

Statistical methods

Summary statistics such as means, medians, standard deviations, ranges, frequencies and proportions were reported to describe participant demographical and clinical characteristics. Wilcoxon rank sum test or Chi-square test was used to compare participant characteristics across pathology groups. Logistic regression model was used to evaluate the correlation between participant characteristics with true positive result for the main data set and subgroup analysis. Subgroup analysis was conducted for participants with mass and non-mass lesions, respectively.

Results

Two-hundred-nineteen cases (median age, 49 years; range, 26–85 years) were included. The indication of MRI before biopsy were screening (n = 106) 48%; staging (n = 63) 29%; surveillance with history of previous malignant lumpectomy (n = 20) 9%; problem solving (n = 13) 6%; and others (n=17) 8%. Out of 219 MRI-guided biopsies, 137 (62.5%) lesions were benign, 39 (18%) malignant, and 43 (19.6%) high-risk.Demographic parameters and imaging findings of the MRI-biopsy lesions withbenign, high risk, and malignant outcomes are summarized in **Table 1**. The flowchart of the patients with MRI-guided biopsy in our center in 2018 is also presented **[Figure 1].**

The false-positive result in our study was 82.2%. **Figures 2–4 s**how examples of false-positive cases.

Table 2 summarizes the univariate analysis's demographic and imaging features associated with malignant outcome. In addition, subgroup analysis for mass lesions and non-mass lesions were performed **[Tables 3 and 4]**

The univariate analysis showed that between a variety of clinical and pathological parameters, age was the only demographic characteristic that showed a significant influence on the differentiation of false-positive and true positive groups. Older women had more chance to have a true positive lesion, *p=0.0015*; OR 1.05 (CI 95%, 1.02 - 1.08).

Out of 219 cases, 41 (19%) of the cases were masses, while 178 (81%) were non-mass. The mass to non-mass lesions ratio was not significant between the true positive (malignant pathology result) and false-positive groups (benign or high-risk pathology result) with a p-value of 0.44.

Indication of MRI (p = 0.22), positive first-degree family history (p = 0.056), previous personal history of breast cancer (p = 0.068), and background parenchymal enhancement (p = 0.075) did not show significant influence on correct diagnosing of true positive lesions.

Tumor diameter had no influence on the correct diagnosis of both mass (p = 0.55) and non-mass lesions (p = 0.4). The mean diameter of false-positive masses was 7.34 mm (SD 1.70) and of true positive masses was 8.67 mm (SD 3.71). The mean diameter of false-positive non-masses was 16.28 mm (SD 15.94), and true positive non-masses was 19.13 mm (SD 16.31).

For masses, compared with oval/round shape, irregular shape significantly increased the ratio of true positive [*p = 0.015*, OR 11.20 (CI 95%, 1.6–78.4)]. In addition, hyperintense signal on the T2-weighted sequence (compared to the normal fibroglandular signal) was significantly related to the false-positive result [*p = 0.024*, OR 0.13 (95% CI, 0.02–0.76)]. Dynamic curve (p = 0.98), T1 signal (p = 0.25), and mass margin (p = 0.2) did not differentiate malignant from benign/high-risk lesions.

In the evaluation of non-mass lesions, the only feature that significantly differentiated malignant and benign/high-risk lesions was enhancement pattern; compared to homogeneous, clumped and clustered ring of enhancement was significantly related to a true positive result, *p < 0.0066*, OR 3.17 (CI 95%, 1.38–7.28). Distribution (p = 0.44), T1 signal (p = 0.77), T2 signal (p = 0.17), and dynamic curve (p = 0.97), did not have significant difference in true positive and false positive groups.

Discussion

The malignancy rate of 18% of MRI-detected lesions in our cohort is slightly lower than the BI-RADS lexicon benchmark of 20–50% [27] and aligns with the lower range of previously published studies, ranging from 18 to 60% [28–36], suggesting that there is no excessive number of biopsies in our institution. However, the high rate of false-positive results in our cohort, while similar to the previously published study focused on screening [37], warrants knowledge of which lesion characteristics are related to the false positive to minimize the cost of health care and the patient's anxiety. In this evaluation, young

patients, oval/round mass-lesion shape, hyperintense mass-lesion on T2 weighted sequences, and homogeneous pattern of non-mass enhancement were the identified variables associated with false-positive results. They may be considered to forego biopsies in the future.

With respect to demographic characteristics, our results showed that lesions in older women had a greater chance of being true positive than false positive. However, the study by Myers et al. [21] did not show an association of age with malignancy (p = 0.43). This discrepancy can be related to the different populations included in the study. Although MRI indication did not show a statistically significant difference in the false positive rate in either study, our study was predominantly in high-risk populations, and Myers focused on breast cancer patients undergoing MRI for disease assessment.

Regarding the lesion features for mass-like lesions, contrary to previously published studies [20, 21], which showed that margin irregular [20] and spiculated [21] were parameters associated with malignancy, our study showed that irregular shape and not margin was the feature associated with malignancy. In fact, the difference in the results may be attributed to both, the small number of irregular shape lesions in our study limiting our statistical power, and the subjective analysis of these characteristics, which can cause possible overlapping between irregular margin and shape in the lesion classification. In addition, similar to Myers' study [21], the hyper signal on the T2-weighted sequence (compared to normal fibroglandular signal) was significantly related to false-positive results.

For non-mass lesions, to the best of our knowledge, this is the first time showing that any clumped and clustered ring of enhancement was significantly related to a true positive result, $p < 0.0066$.

Moreover, although a smaller number of high-risk lesions (24%, 43/180) were identified in our cohort compared to previously published study (44.8%, 81/202) [11], the rate of a high-risk lesion identified cannot be neglected considering its prognostic importance, which can reflect in different patient's management including intensified surveillance, preventive surgery, or even chemoprevention.

Avoiding biopsy of MRI-detected lesions with features related to the false-positive rate can potentially decrease healthcare cost and patient anxiety. Therefore, it is the main strength of our study.

However, there are several limitations. The main limitation lies in its retrospective design, which may be subject to selection bias. In this sense, the study design, excluding lesions for which biopsy was not recommended (findings that could be true negative or false negative), may have caused over or underestimation of certain characteristics of the lesion associated with benign or malignant results. Secondly although the MRI data were reviewed by two breast-trained radiologists and the discrepant results of lesion characteristics among radiologists were assessed by consensus, lesion classification based on subjective parameters defined by the BI- RADS can affect false-positive rates limiting the generalizability of results. In this sense, application of AI technology may surpass this subjectively assessment, providing a more reliable, objective way to differentiate benign and malignant lesions. Nevertheless, such applications are still in the technical development phase and are far from being incorporated into clinical practice [22–24, and 38].Third, MRI technology has evolved and proton MR

spectroscopy and diffusion weighting can also affect false-positive results. However, these techniques require a longer acquisition time and have a substantial number of technical flaws, such as voxel shift, incomplete acquisition, or incorrect shimming, and therefore, their performance was not evaluated in our study [39, 40]. Last but not least, false positives may be affected depending on the indication of the MRI study, and therefore, our study focused primarily on high-risk patients may not be transferable to other settings.

Conclusion

Based on our result, young patients, oval/round mass-lesion shape, and homogeneous pattern of non-mass enhancement showed the strongest association with false-positive results of incidental enhancing lesions depicted by MRI. For participants with mass breast lesion, T2-hyperintense mass-lesion showed significant association with false-positive result. It may impact the patient's management with a suggestion of follow-up rather than interventional procedure when these demographic and imaging parameters are present, consequently decreasing the patient's anxiety and health care costs until upcoming new technologies including AI can be incorporated into the clinical practice to allow us reliably differentiate benign and malignant lesions, minimizing unnecessary biopsies, improving work flow and decreasing health care costs.

References

1. Kuhl CK, Weigel S, Schrading S et al (2010) Prospective Multicenter Cohort Study to Refine Management Recommendations for Women at Elevated Familial risk of Breast Cancer: The EVA Trial. J Clin Oncol 28(9):1450–1457
2. Lehman CD, Isaacs C, Schnall MD et al (2007) Cancer yield of mammography, MR, and US in high-risk women: prospective multi-institution breast cancer screening study. Radiology 244(2):381–388
3. Sardanelli F, Podo F, D'Agnolo G et al (2007) High Breast Cancer Risk Italian Trial. Multicenter comparative multimodality surveillance of women at genetic-familial high risk for breast cancer (HIBCRIT study): interim results. Radiology 242(3):698–715
4. Sung JS, Lee CH, Morris EA, Oeffinger KC, Dershaw DD (2011) Screening breast MR imaging in women with a history of chest irradiation. Radiology 259(1):65–71
5. Freitas V, Scaranelo A, Menezes R, Kulkarni S, Hodgson D, Crystal P (2013) Added cancer yield of breast magnetic resonance imaging screening in women with a prior history of chest Radiation therapy. Cancer Feb1:119(3):495–503
6. Mendelson EB, Berg WA (2015) Training and standards for performance, interpretation, and structured reporting for supplemental breast cancer screening. AJR Am J Roentgenol 204:265–268
7. Health Quality Ontario (2016) Magnetic resonance imaging as an adjunct to mammography for breast cancer screening in women at less than high risk for breast cancer: a health technology assessment. Ont Health Technol Assess Ser 16(20):1–30

8. Kuhl CK, Strobel K, Bieling H, Leutner C, Schild HH, Schrading S (2017) Supplemental breast MR imaging screening of women with average risk of breast cancer. Radiology 283:361–370
9. Kuhl CK (2018) Abbreviated breast MRI for screening women with dense breast: the EA1141 Trial. Br J Radiol 91(1090):20170441
10. Bakker MF et al (2019) Supplemental MRI Screening for Women with Extremely Dense Breast Tissue. N Engl J Med 381(22):2091–2102
11. Kuhl CK, Keulers A, Strobel K et al (2018) Not all false positive diagnoses are equal: On the prognostic implications of false positive diagnoses made in breast MRI versus in mammography / digital tomosynthesis screening. Breast Cancer Res 20:13
12. Van Zee KJ, Barrio AV, Tchou J, Society of Surgical Oncology Breast Disease Site Work Group (2016) Treatment and long-term risks for patients with a diagnosis of ductal carcinoma in situ. JAMA Oncol 2:397–398
13. Dabbous FM, Dolecek TA, Berbaum ML et al (2017) Impact of a false-positive screening mammogram on subsequent screening behavior and stage at breast cancer diagnosis. Cancer Epidemiol Biomarkers Prev 26:397–403
14. Hardesty LA, Lind KE, Gutierrez EJ (2016) Compliance with screening mammography guidelines after a false-positive mammogram. J Am Coll Radiol 13:1032–1038
15. Román M, Castells X, Hofvind S, von Euler-Chelpin M (2016) Risk of breast cancer after false-positive results in mammographic screening. Cancer Med 5:1298–1306
16. Nelson HD, Pappas M, Cantor A, Griffin J, Daeges M, Humphrey L (2016) Harms of breast cancer screening: systematic review to update the 2009 U.S. Preventive Services Task Force recommendation. Ann Intern Med 164:256–267
17. Melnikow J, Fenton JJ, Whitlock EP et al (2016) Supplemental screening for breast cancer in women with dense breasts: a systematic review for the U.S. Preventive Service Task Force. Report no. 14-05201-EF-3. Agency for Healthcare Research and Quality, Rockville, MD
18. Menezes GL, Knuttel FM, Stehouwer BL, Pijnappel RM, van den Bosch MA (2014) Magnetic resonance imaging in breast cancer: a literature review and future perspectives. World J Clin Oncol 5:61–70
19. Sardanelli F, Boetes C, Borisch B et al (2010) Magnetic resonance imaging of the breast: recommendations from the EUSOMA working group. Eur J Cancer 46:1296–1316
20. Pascal AT, Baltzer M, Benndorf M, Dietzel et al (2010) False-Positive Findings at Contrast-Enhanced Breast MRI: A BI-RADS Descriptor Study. Am J Roentgenol 194(6):1658–1663
21. Myers KS, Kamel IR, Macura KJ (2015) MRI-guided breast biopsy: outcomes and effect on patient management. Clin Breast Cancer 15(2):143–152
22. Codari M, Schiaffino S, Sardanellia F (2019) Rubina Manuela Trimboli. Artificial Intelligence for Breast MRI in 2008–2018: A Systematic Mapping Review. Am J Roentgenol 212:280–292. 10.2214/AJR.18.20389

23. Dong-Man Ye MD1, Wang H-T, Yu T (2020) Ph. The Application of Radiomics in Breast MRI: A Review. Technol Cancer Res Treat Jan-Dec 19:1533033820916191. doi: 10.1177/1533033820916191
24. Reig B (2021 Aug) Radiomics and deep learning methods in expanding the use of screening breast MRI. Eur Radiol 31(8):5863–5865. doi: 10.1007/s00330-021-08056-9. Epub 2021 May 20. PMID: 34014381
25. ACR Practice Parameter for the Performance of Contrast Enhanced Magnetic Resonance Imaging (MRI) of the Breast (2018) https://www.acr.org/-/media/acr/files/practice-parameters/mr-contrast-breast.pdf. Assessed January 07, 2022
26. American College of Radiology. BI-RADS: MRI (2013) Breast imaging reporting and data system: BI-RADS atlas. American College of Radiology, Reston, VA
27. Sickles EA, D'Orsi CJ (2013) ACR BI-RADS follow-up and outcome monitoring. ACR BI-RADS Atlas, Breast Imaging Reporting and Data System. American College of Radiology, Reston, Va
28. Mahoney MC (2008) Initial clinical experience with a new MRI vacuum-assisted breast biopsy device. J Magn Reson Imaging 28:900–9054
29. Orel SG, Rosen M, Mies C, Schnall MD (2006) MR imaging-guided 9-gauge vacuum-assisted core-needle breast biopsy: initial experience. Radiology 238:54–615
30. Lehman CD, Deperi ER, Peacock S, McDonough MD, Demartini WB, Shook J (2005) Clinical experience with MRI-guided vacuum-assisted breast biopsy. AJR 184:1782–1787
31. Liberman L, Morris EA, Dershaw DD, Abramson AF, Tan LK (2003) MR imaging of the ipsilateral breast in women with percutaneously proven breast cancer. AJR Am J Roentgenol 180(4):901–910
32. Perlet C, Heywang-Kobrunner SH, Heinig A et al (2006) Magnetic resonance-guided, vacuum-assisted breast biopsy: results from a European multicenter study of 538 lesions. Cancer 106:982–990
33. Han BK, Schnall MD, Orel SG, Rosen M (2008) Outcome of MRI-guided breast biopsy. AJR 191:1798–1804
34. Liberman L, Bracero N, Morris E, Thornton C, Dershaw DD (2005) MRI-guided 9-gauge vacuum-assisted breast biopsy: initial clinical experience. AJR 185:183–193
35. Malhaire C, El Khoury C, Thibault F et al (2010) Vacuum-assisted biopsies under MR guidance: results of 72 procedures. Eur Radiol 20:1554e–1562e
36. Rauch GM, Dogan BE, Smith TB, Liu P, Yang WT (2012) Outcome analysis of 9-gauge MRI-guided vacuum-assisted core needle breast biopsies. AJR Am J Roentgenol 198(2):292–299
37. Hoogerbrugge N, Kamm YJL, Bult P (2008) The impact of a false-positive MRI on the choice for mastectomy in BRCA mutation carriers. Ann Oncol 19:655–659
38. Jiang Y, Edwards AV, Newstead GM (2021 Jan) Artificial Intelligence Applied to Breast MRI for Improved Diagnosis. Radiology 298(1):38–46. doi: 10.1148/radiol.2020200292. Epub 2020 Oct 20. PMID: 33078996

39. Sharma U, Jagannathan NR (2022) Magnetic Resonance Imaging (MRI) and MR Spectroscopic Methods in Understanding Breast Cancer Biology and Metabolism. Metabolites 12:295. https://doi.org/10.3390/metabo12040295
40. Fardanesh R, Marino MA, Avendano D, Leithner D, Pinker K, Thakur SB (2019) Proton MR spectroscopy in the breast: Technical innovations and clinical applications. J Magn Reson Imaging 50:1033–1046. https://doi.org/10.1002/jmri.26700

Tables

Table 1. Demographic parameters and imaging findings of the MRI-biopsy lesions with benign, high risk and malignant

Covariate	Full Sample (n=219)	Benign (n=137)	High-risk lesion (n=43)	Malignant (n=39)	p-value
Age (years)					**0.0015**
Mean (sd)	49.7 (12.2)	47.6 (11.9)	51.1 (12.1)	55.5 (11.5)	
Median (Min, Max)	49 (26,85)	46 (26,79)	52 (26,78)	53 (36,85)	
Genetic mutation					0.42
Yes	13 (6)	7 (5)	2 (5)	4 (10)	
No	206 (94)	130 (95)	41 (95)	35 (90)	
Family History of BC					**0.043**
Yes	98 (45)	70 (51)	16 (37)	12 (31)	
No	121 (55)	67 (49)	27 (63)	27 (69)	
Personal History of BC					0.082
Y	100 (46)	55 (40)	22 (51)	23 (59)	
N	119 (54)	82 (60)	21 (49)	16 (41)	
Personal History of BC: Remote or Newly Diagnosed BC					0.88
Newly Diagnosed	62 (61)	34 (60)	13 (59)	15 (65)	
Remote	40 (39)	23 (40)	9 (41)	8 (35)	
Missing	**117**	**80**	**21**	**16**	
Newly diagnosed BC: ipsilateral or contralateral					0.09
Ipsilateral	42 (41)	22 (39)	8 (36)	12 (52)	
Contralateral	58 (57)	35 (61)	14 (64)	9 (39)	
Bilateral	2 (2)	0 (0)	0 (0)	2 (9)	
Missing	**117**	**80**	**21**	**16**	
Indication					0.04
Screening	105 (48)	74 (54)	17 (40)	14 (36)	
Staging	63 (29)	33 (24)	15 (35)	15 (38)	
Surveillance	20 (9)	12 (9)	4 (9)	4 (10)	
Problem-Solving	13 (6)	11 (8)	2 (5)	0 (0)	

Other	17 (8)	6 (4)	5 (12)	6 (15)	
Missing	**1**	**1**	**0**	**0**	
MRI BPE					0.03
Minimal-mild	176 (81)	110 (81)	31 (72)	35 (90)	
Moderate	37 (17)	25 (18)	10 (23)	2 (5)	
Marked	5 (2)	1 (1)	2 (5)	2 (5)	
Missing	**1**	**1**	**0**	**0**	
Breast Lesion: Mass or NME					0.19
Mass	41 (19)	28 (20)	4 (9)	9 (23)	
NME	178 (81)	109 (80)	39 (91)	30 (77)	
Mass Lesion Shape					0.03
Oval/round	33 (85)	24 (92)	4 (100)	5 (56)	
Irregular	6 (15)	2 (8)	0 (0)	4 (44)	
Missing	**180**	**111**	**39**	**30**	
Distribution of NME					0.003
focal/focus	105 (58)	71 (64)	18 (46)	16 (53)	
ductal/linear	44 (24)	19 (17)	18 (46)	7 (23)	
segmental	13 (7)	9 (8)	2 (5)	2 (7)	
regional	16 (9)	12 (11)	0 (0)	4 (13)	
multiple regional	1 (1)	0 (0)	0 (0)	1 (3)	
Diffuse	1 (1)	0 (0)	1 (3)	0 (0)	
Missing	**39**	**26**	**4**	**9**	
NME pattern					0.02
homogeneous	135 (75)	89 (80)	29 (74)	17 (57)	
heterogeneous	4 (2)	4 (4)	0 (0)	0 (0)	
clumped	40 (22)	18 (16)	9 (23)	13 (43)	
clustered ring	1 (1)	0 (0)	1 (3)	0 (0)	
Missing	**39**	**26**	**4**	**9**	
T2 signal					0.28

hyper	61 (28)	40 (29)	13 (30)	8 (21)	
No	119 (54)	70 (51)	21 (49)	28 (72)	
intermediate	38 (17)	26 (19)	9 (21)	3 (8)	
low	1 (0)	1 (1)	0 (0)	0 (0)	
T1 signal					0.50
No	165 (75)	100 (73)	36 (84)	29 (74)	
Low & Iso	50 (23)	34 (25)	6 (14)	10 (26)	
Hyper	4 (2)	3 (2)	1 (2)	0 (0)	
Size (mm)					0.27
Mean (sd)	15.1 (14.9)	14.1 (14.4)	16.5 (16.4)	16.7 (15)	
Median (Min,Max)	9 (3,100)	8 (4,71)	11 (4,100)	10 (3,60)	
Dynamic curve					0.44
persistent	82 (37)	54 (39)	15 (35)	13 (33)	
plateau	34 (16)	22 (16)	7 (16)	5 (13)	
wash out	69 (32)	44 (32)	10 (23)	15 (38)	
mixed	34 (16)	17 (12)	11 (26)	6 (15)	

BC = breast cancer; BPE = background parenchymal enhancement; NME = non-mass enhancement

Table 2 – Univariate analysis - Demographic and imaging features associated with malignant outcome

Covariate	OR(95%CI)	p-value	Global p-value
Age	1.05 (1.02,1.08)		**0.0015**
gene mutation			0.22
Yes	Reference		
No	0.46 (0.13,1.58)		
Family HX			0.056
Yes	Reference		
No	2.06 (0.98,4.32)		
Personal HX			0.068
Y	Reference		
N	0.52 (0.26,1.05)		
same or contralateral			0.3
Ipsilateral	Reference		
Contralateral	0.46 (0.17,1.22)	0.12	
Bilateral	0.00 (0,Inf)	0.99	
Simultaneous or Metachronous			0.62
Synchronous	Reference		
Metachronous	0.78 (0.30,2.06)		
Indication			0.22
Screening	Reference		
Staging	2.03 (0.91,4.56)	0.086	
Surveillance	1.62 (0.47,5.57)	0.44	
Problem-Solving	0.00 (0,Inf)	0.99	
Other	3.55 (1.13,11.12)	**0.03**	
MRI BPE			0.075
Minimal-mild	Reference		
Moderate	0.23 (0.05,1.00)	0.051	
Marked	2.69 (0.43,16.69)	0.29	
breast Lesion: Mass/NME			0.44

Mass	Reference		
NME	0.72 (0.31,1.66)		
Size	1.01 (0.99,1.03)		0.44
Mass border/margin			0.2
Regular	Reference		
Irregular	4.00 (0.48,33.58)		
Mass shape			**0.015**
Oval/round	Reference		
Irregular	11.20 (1.60,78.40)		
NME pattern			**0.022**
homogeneous	Reference		
heterogeneous	0.00 (0,Inf)	0.99	
clumped/clustered ring	3.22 (1.40,7.40)	**0.0058**	
NME Distribution			0.42
focal/focus	Reference		
ductal/linear/segmental	1.04 (0.43,2.54)	0.93	
regional/multiple regional/Diffuse	2.14 (0.67,6.83)	0.2	
T1 signal			0.93
No	Reference		
Low & Iso	1.17 (0.53,2.61)	0.7	
Hyper	0.00 (0,Inf)	0.99	
T2 signal			0.053
No	Reference		
low/intermediate	0.27 (0.08,0.95)	**0.041**	
hyper	0.49 (0.21,1.15)	0.1	
dynamic curve			0.76
persistent	Reference		
plateau	0.92 (0.30,2.80)	0.88	
wash out	1.47 (0.65,3.36)	0.36	

mixed	1.14 (0.39,3.29)	0.81

Note: Odds ratio (OR) is a measure of association between a variable and an binary outcome (false positive vs true positive). OR>1 indicates increased occurrence of true positive while OR <1 indicates decreased occurrence of true positive. P value<0.05 indicates the estimated OR is significantly different from 1.

Table 3 – Univariate analysis - Subgroup analysis for Mass lesions

3.1 Summary table of tumor size between false positive and true positive groups for Mass lesions

Covariate	Full Sample (n=41)	FP (n=32)	TP (n=9)	p-value
Size				0.55
Mean (sd)	7.63 (2.30)	7.34 (1.70)	8.67 (3.71)	
Median (Q1,Q3)	7 (6,9)	7 (6,9)	7 (6,12)	
Range (min, max)	(4,15)	(5,11)	(4,15)	

Note: P=0.55>0.05, indicating that size is not significantly associated with correct diagnose for mass region.

3.2 Summary table of mass characteristics between false positive and true positive groups for Mass lesions

Covariate	OR(95%CI)	p-value	Global p-value
Size	1.27 (0.92,1.74)		0.14
Mass border/margin			0.2
Regular	Reference		
Irregular	4.00 (0.48,33.58)		
Mass shape			**0.015**
Oval/round	Reference		
Irregular	11.20 (1.60,78.40)		
T1 signal			0.25
No	Reference		
Low & Iso	0.37 (0.07,1.99)		
T2 signal			**0.04**
No	Reference		
low/intermediate	0.09 (0.0077,1.03)	0.053	
hyper	0.13 (0.02,0.76)	**0.024**	
dynamic curve			0.98
persistent	Reference		
plateau	0.00 (0,Inf)	0.99	
wash out	1.47 (0.25,8.70)	0.67	
mixed	0.00 (0,Inf)	1	

3.3 Subgroup analysis for Mass shape (n=33)

Covariate	OR(95%CI)	p-value	Global p-value
Size	0.73 (0.38,1.41)		0.35
T1 signal			0.74
No	Reference		
Low & Iso	0.67 (0.06,7.60)		
T2 signal			0.18
No	Reference		
low/intermediate	0.11 (0.0064,1.92)	0.13	
hyper	0.12 (0.01,1.36)	**0.087**	
dynamic curve			0.85
persistent	Reference		
plateau	0.00 (0,Inf)	1	
wash out	2.00 (0.19,20.97)	0.56	

3.4 Subgroup analysis for Mass margin (n=35)

Covariate	OR(95%CI)	p-value	Global p-value
Size	1.03 (0.66,1.62)		0.89
T1 signal			0.38
No	Reference		
Low & Iso	0.42 (0.06,2.93)		
T2 signal			0.096
No	Reference		
low/intermediate	0.07 (0.0048,1.14)	0.062	
hyper	0.12 (0.01,1.03)	0.053	
dynamic curve			0.97
persistent	Reference		
plateau	0.00 (0,Inf)	0.99	
wash out	1.25 (0.20,7.92)	0.81	

Table 4. Subgroup analysis for Non-mass lesions

4.1 Summary table of tumor size between false positive and true positive groups for Non-Mass lesions

Covariate	Full Sample (n=178)	FP (n=148)	TP (n=30)	p-value
Size				0.4
Mean (sd)	16.76 (15.99)	16.28 (15.94)	19.13 (16.31)	
Median (Q1,Q3)	10 (6,22)	10.00 (6.00,21.25)	12.50 (7.00,29.50)	
Range (min, max)	(3,100)	(4,100)	(3,60)	

Note: P=0.4>0.05, indicating that size is not significantly associated with correct diagnose for non-mass region.

4.2 Summary table of mass characteristics between false positive and true positive groups for Non-Mass lesions

Covariate	OR(95%CI)	p-value	Global p-value
Size	1.01 (0.99,1.03)		0.37
NME pattern			**0.025**
homogeneous	Reference		
heterogeneous	0.00 (0,Inf)	0.99	
clumped/clustered ring	3.17 (1.38,7.28)	**0.0066**	
NME Distribution			0.44
focal/focus	Reference		
ductal/linear/segmental	1.02 (0.42,2.48)	0.97	
regional/multiple regional/Diffuse	2.09 (0.65,6.68)	0.21	
T1 signal			0.77
No	Reference		
Low & Iso	1.55 (0.47,5.13)	0.47	
Hyper	0.00 (0,Inf)	0.99	
T2 signal			0.17
No	Reference		
low/intermediate	0.28 (0.06,1.27)	0.098	
hyper	0.56 (0.20,1.58)	0.27	
dynamic curve			0.97
persistent	Reference		
plateau	1.11 (0.35,3.52)	0.86	
wash out	1.27 (0.47,3.45)	0.64	
mixed	1.23 (0.41,3.68)	0.71	

NME – non-mass enhancement

Figures

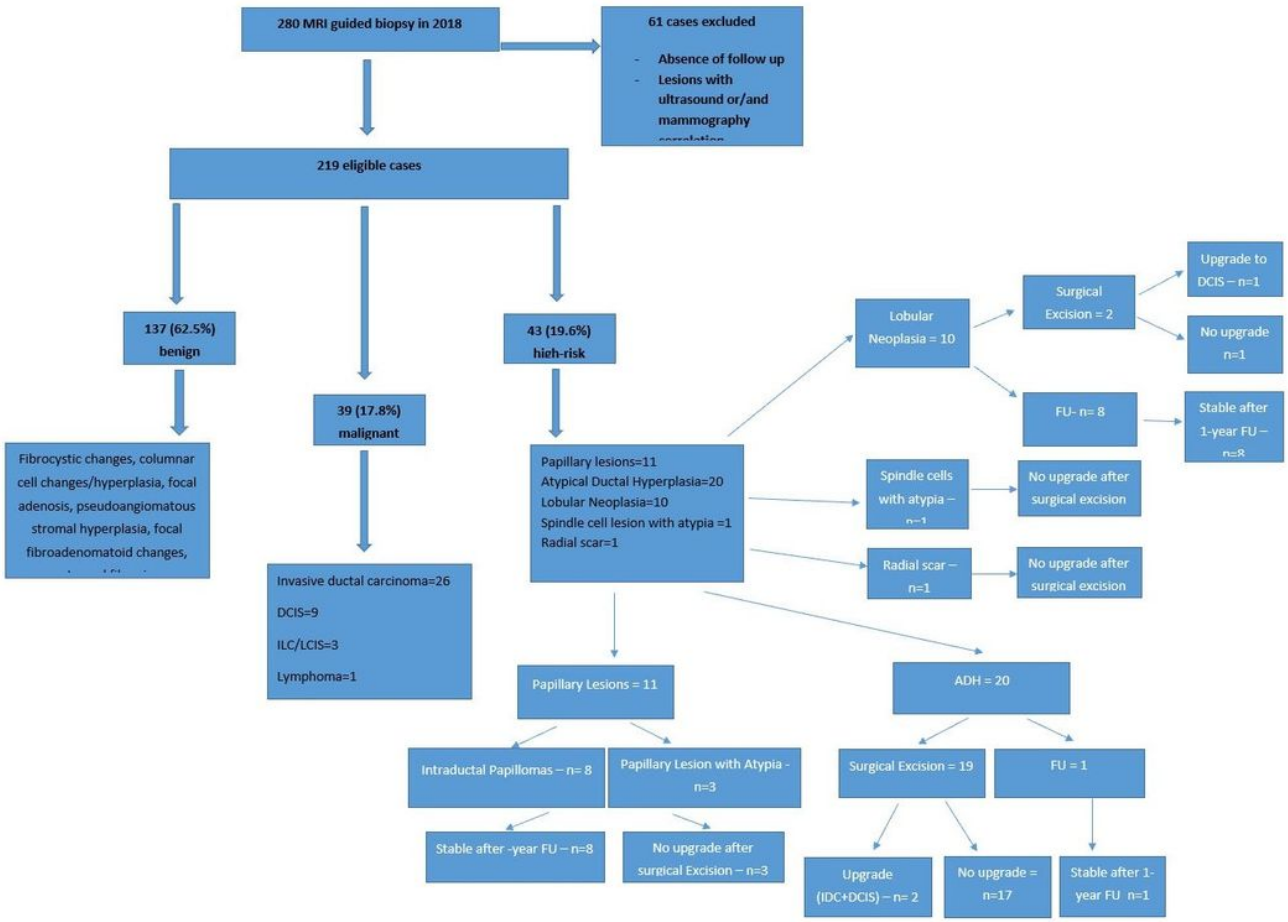

Figure 1

Flowchart of the lesions with MRI-guided biopsy

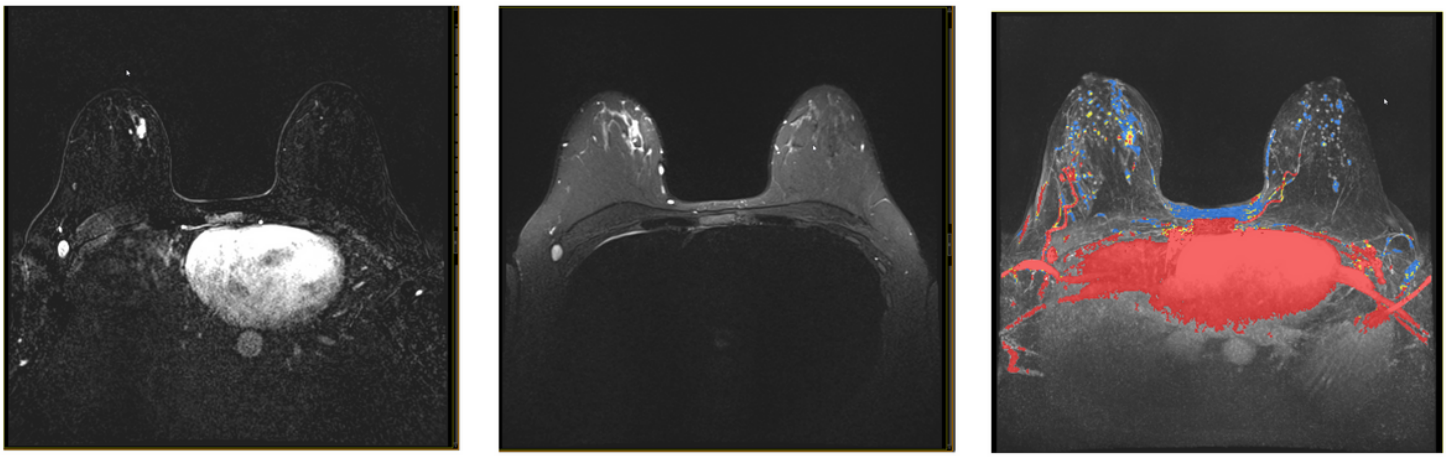

a b c

Figure 2

A 40-year-old woman, high-risk. Axial, fat-saturated, contrast-enhanced, and subtracted T1-weighted images show (a) homogeneously enhancing mass in the upper inner quadrant (arrow) (b) bright on T2-weighted sequence (arrow) (c) with mixed included washout kinetics on the post-processing color map (arrow). No mammography and ultrasound correlate was detected, and MRI-guided biopsy was performed. Pathology reported fragments of benign breast tissue showing fibrocystic changes, columnar cell changes/hyperplasia, and focal mild to moderate ductal hyperplasia, duct ectasia, and focal chronic inflammation with histiocytic and reactive changes suggestive of reaction to cyst/duct rupture.

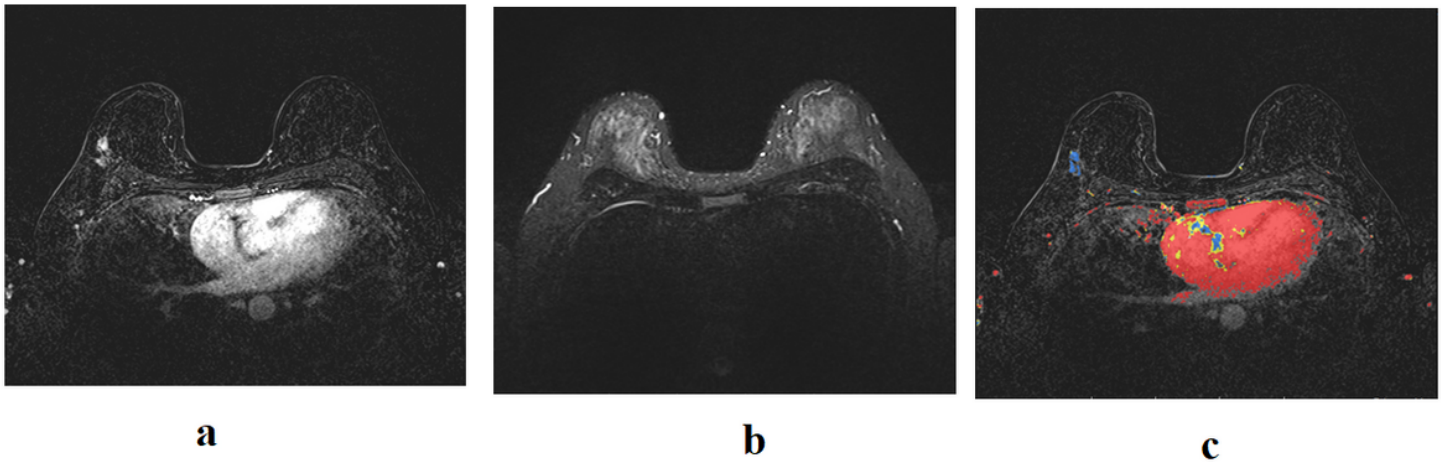

Figure 3

A 44-year-old woman, high-risk. Axial, fat-saturated, contrast-enhanced, and subtracted T1-weighted images show (a) a developing heterogeneous focal non-mass enhancement in the right upper outer quadrant (b) with intermediate signal on T2-weighted sequence (c) and persistent kinetics. It underwent MRI-guided biopsy. The pathology result yielded unremarkable breast tissue with pseudoangiomatous stromal hyperplasia.

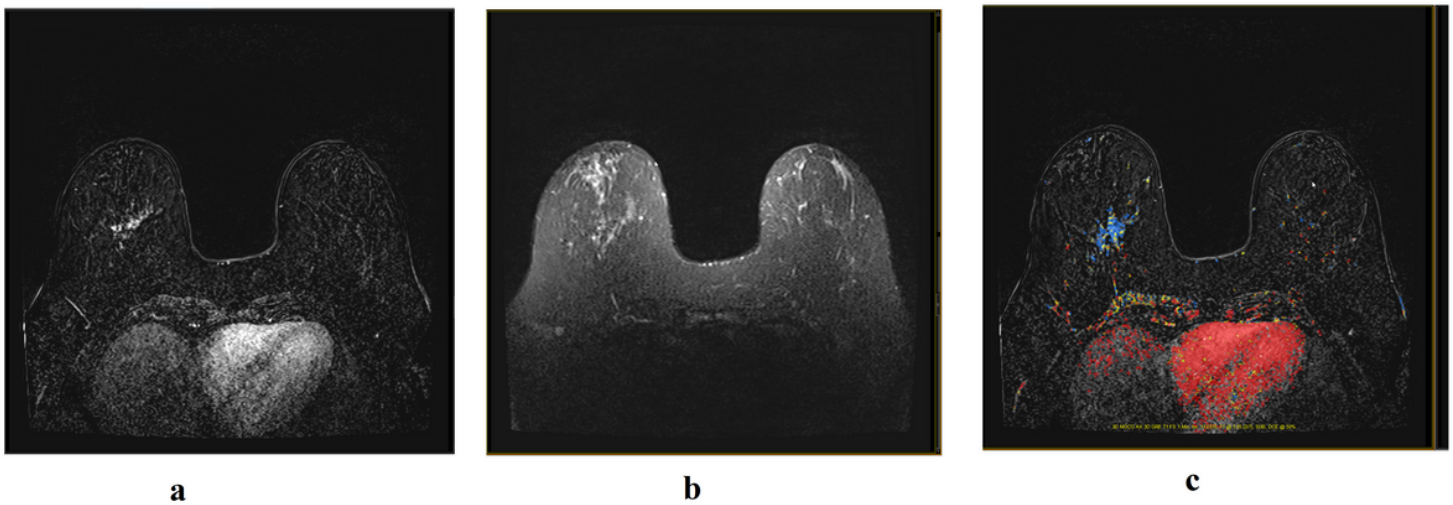

Figure 4

A 52-year-old woman, high-risk. Axial, fat-saturated, contrast-enhanced, and subtracted T1-weighted images show (a) a focal area of non-mass enhancement in the inferior right breast (b) with intermediate signal on T2-weighted sequence (c) and mixed kinetics, including washout. It underwent MRI-guided biopsy. The pathology result was atypical ductal hyperplasia and atypical lobular hyperplasia with duct involvement by cells of atypical lobular hyperplasia.